Title: A diagnostic relationship between the RNA Integrity Number equivalent and Time Since Deposition of blood

Authors: Colin I. Elliott[a*], Theresa E. Stotesbury[b], Aaron B.A. Shafer[a,c]

[a] Department of Forensic Science, Trent University, 1600 West Bank Drive, Peterborough, ON, K9L 0G2, Canada

[b] Faculty of Science, Forensic Science, Ontario Tech University, 2000 Simcoe St N, Oshawa, ON, L1G 0C5, Canada

[c] Environmental and Life Sciences Graduate Program, Trent University, 1600 West Bank Drive, Peterborough, ON, K9L 0G2, Canada

* **Corresponding author:** colinelliott@trentu.ca

Highlights

- Total RNA degradation data for bloodstain time since deposition.
- RNA quality and concentration are correlated to time.
- Diagnostic drop in RNA quality metric after 24 hours.
- Biological replicates produced similar results for an RNA quality metric.
- Use of automated high-sensitivity gel electrophoresis for analysis.

Abstract

Determining the age, or time since deposition (TSD), of bloodstains would provide forensic scientists with critical information regarding the timeline of the events of bloodshed during a crime. The physicochemical changes that occur to major biomolecules as a bloodstain dries can be used to estimate the TSD of bloodstains. For example, high-resolution automated gel electrophoresis can be used to quantify the timewise degradation of DNA present in bloodstains. Our study aims to analyze and quantify the timewise degradation trends found in total RNA from bloodstains, expanding the scope of the TSD research which has previously explored DNA and targeted mRNA molecules. Fifty bloodstains were stored in plastic microcentrifuge tubes at room temperature and tested over 10 different timepoints spanning one week. A total of eight RNA metrics were visually assessed and quantified using linear regression. RNA Integrity Number equivalent (RINe), total RNA concentration, and 28S/18S rRNA peak area ratios were retained for further analyses based on their relationship with time and limited correlations. RINe and total RNA concentration both exhibited negative trends over time, highlighting a decrease in quality and quantity. RINe was the RNA metric that

demonstrated the greatest association with time (R^2 = 0.696). Generalized linear mixed-effects models including donor (biological replicate) as a random effect increased the fit for all RNA metrics to varying degrees, but no significant differences were found between biological replicates for the RINe metric. Our results illustrated the presence of a significant decrease in the retained RNA metrics after 24 hours, suggesting that this method could be used to reliably differentiate day-old bloodstains from older bloodstains. Future work should focus on recreating this study in different environmental conditions, including testing on a variety of substrates.

Keywords

Time Since Deposition, total RNA, RNA Integrity Number equivalent, bloodstain, electrophoresis

1. Introduction

Accurate determination of the time at which a crime occurred remains a challenge in forensic investigations [1,2]. Bloodstains are common types of biological evidence found at crime scenes involving bloodshed, and determining their age, or time since deposition (TSD), would provide context in criminal investigations, including the development of investigative leads and the assessment of alibis [1–4]. Currently, blood at crime scenes is subjected to bloodstain pattern analysis (BPA), which provides potential interpretations of the physical events that gave rise to the bloodshed [5]. Deoxyribonucleic acid (DNA) profiling, used for attribution purposes, can also be carried out using crime scene bloodstains [6–8]. Although

72 useful in their own ways, none of these tools help with determining the exact timing of the
73 event, specifically *when* the crime might have occurred. Previous studies have developed
74 chemometric [2,9–11] and genetic methodologies [3,12–14] that estimate the TSD of
75 bloodstains in controlled laboratory conditions. To this date, these methods have not been
76 accepted for field use, as they largely exhibit insufficient sensitivity and specificity, and high
77 variability between samples and crime scene conditions [3,9–13,15].

78 *Ex-vivo*, blood undergoes a series of time-dependent physicochemical and
79 morphological changes, such as hemoglobin oxidation and conformational changes [10,16],
80 drying [17,18], clotting [19,20], and DNA and ribonucleic acid (RNA) degradation [3,21–24]. RNA
81 degradation, specifically total RNA degradation, has not been studied as extensively as
82 individual mRNA molecules [25]. RNA in blood originates from leukocytes, commonly referred
83 to as white blood cells [1]. RNA is a single-stranded nucleic acid that can fold on itself to create
84 double-stranded secondary and tertiary structures [26]. It contains a uracil nitrogenous base
85 rather than a thymine base, and a ribose sugar, rather than a deoxyribose sugar [26]. Total RNA,
86 all the RNA in a cell, encompasses ribosomal RNAs (rRNA), messenger RNAs (mRNA), transfer
87 RNAs (tRNA) and microRNAs (miRNA), among others [27]. Eukaryotic rRNA makes up for 80% of
88 the total RNA in a cell and consists of 5S, 5.8S, 18S and 28S rRNA [28].

89 To circumvent potential PCR inhibition from the heme in blood and the stochastic
90 effects and amplification biases caused by reverse transcriptase and PCR [29–31], our approach
91 focused on total RNA rather than mRNA. Total RNA degradation can be observed by examining
92 the differently sized fragments with highly sensitive RNA electrophoresis, similar to how
93 Cossette *et al*. quantified DNA concentration in base-pair size bins [24]. Processes that can

induce degradation in RNA can be endogenous or exogenous [25]. Ribonucleases (RNases) are ubiquitously present enzymes that cleave the phosphodiester bonds of RNA [32], increasing the presence of small RNA fragments, and are found on most surfaces, human skin, and airborne dust particles [33,34]. Further, and of particular relevance to forensic studies, RNases are more effective in cleaving their targets in hydrated environments [25]. Therefore, special care must be taken to minimize this type of contamination, especially when the bloodstains are still wet [35]. Additionally, reactive oxygen species (ROS), alkylating agents and ultraviolet (UV) irradiation can cause oxidative damage to RNA nucleotides [36,37]. UV irradiation can also induce crosslinking and unspecified chain breaks in RNA [37]. RNA does undergo less base-pairing than DNA, but all these forms of damage disrupt the base-pairing that occurs in tRNA and rRNA [36]. Other exogenous factor, such as humidity [38,39], pH [40] and temperature [39,41] can also increase RNA degradation.

mRNA expression patterns have been used to identify body fluids found at crime scenes [42,43]. Each cell type found within a bodily fluid, or within a particular tissue generally has a unique gene expression pattern [42]. mRNAs found in one cell type may be absent in another; alternatively, mRNAs can be present in cells with differing amounts [42]. Therefore, a pattern of gene expression obtained via reverse transcriptase quantitative polymerase chain reaction (RT-qPCR) or RNA-seq can be associated with a specific type of body fluid [42,43]. Not only can RNA identify body fluids, its degradation in forensically relevant stains, such as blood, may also correlate with time [44]. Fu *et al.* [14] found that, when analyzing blood specific mRNA transcripts with qPCR, TSD for bloodstains less than 6 months old could be estimated to within a period of 2 to 4 weeks, while bloodstains aged for 6 months to 1 year old could be estimated

to within a period of 4 to 6 weeks. Further, Heneghan *et al.* [39] expanded on the aforementioned study and examined the degradation of three blood-specific transcripts under nine different environmental conditions. Higher temperatures and greater relative humidity accelerated RNA degradation; however, no age estimates were made due to the high variance within the data [39]. Anderson *et al.* [3] also analyzed mRNA transcripts and were able to distinguish 6 days old blood from fresh and aged (30 days) blood. Using rhythmic biomarkers, which are mRNAs that vary according to the time of day, alongside melatonin and cortisol levels, Lech *et al.* [12] were able to classify bloodstains as having been deposited across three time of day periods with high prediction accuracy. Recent high throughput sequencing (HTS) research by Weinbrecht *et al.* [13] demonstrated that the abundance of mRNA transcripts does decrease over time, with blood-specific transcripts detected for up to 12 months.

This study aims to explore the use of total RNA degradation in bloodstain TSD models. To do so, we examined and analyzed the changes in the RNA concentration and quality metrics of total RNA over time in a controlled environment. We hypothesized that the concentration of total RNA in the blood samples will decrease with a longer TSD due to the activity of exogenous RNases [25,32] and the deformation of white blood cells as the blood dries [45,46]. We also hypothesized that quality metrics, such as the RNA Integrity Number equivalent (RINe) and the 28S/18S peak ratio, will decrease over time due to fragmentation of larger RNA fragments and an increase of smaller RNA fragments [32]. Further, for both concentration and quality metrics, we predicted that the greatest decrease would occur before the complete drying of the bloodstain, as the blood still represents a hydrated environment, permitting greater degradation of larger fragments, namely 18S and 28S rRNA, via ubiquitously present RNases

[25]. If this occurs, it will provide greater resolution for early time periods than previous models that have focused on DNA [23,24], as DNA is more resistant to degradation than RNA [25]. Lastly, we also predicted that there will be no detectable RNA extracted from the blood deposited 168 hours due to the enzymatic action of RNases and environmental contamination, causing further degradation to the RNA. Previous studies have shown that mRNA persists longer than 168 hours [3,39]; however, without the aid of PCR amplification, we do not expect to detect total RNA at this point.

2. Methods

2.1 Blood sample collection and deposition

Pathogen-free bovine blood was collected from Otonabee Meat Packers, an abattoir in Peterborough, Ontario, Canada. Bovine blood has previously been optimized for forensic research when acid dextrose anticoagulant solution A (ACD-A) is added at a concentration of 12.5 % v/v, as it exhibits similar fluid properties to that of human blood [47]. Blood treated with ACD anticoagulants have demonstrated better nucleic acid extraction efficiencies than heparin-based anticoagulants and have not been shown to affect the cell counts of the different blood components [48]. The ACD-A used in this study was made by dissolving 6.6 grams of sodium citric dextrose, 2.4 grams of citric acid and 6.68 grams of dextrose anhydrous, all purchased from ACP Chemicals Inc., in 500 mL of distilled water. We collected the bovine blood in an amber Nalgene bottle, which was subsequently placed on ice for transportation back to the laboratory (approximately 15 minutes).

We immediately pipetted 50 µl of blood into plastic microcentrifuge tubes. Each sample was stored at room temperature in 1.5 ml microcentrifuge tubes with open lids for a

designated amount of time before the RNA extraction. We performed two time-series experiments; blood from a different cow (donor) was used for each of them. In the first, RNA extractions were completed at 0 hours (time of initial pipetting), 1.5, 3, 6, 9, 24,48, 72, 96, and 168 hours after sample deposition. In the second, we replaced the 168-hour timepoint with a 36-hour timepoint to better characterize the observed decrease in RNA quality and concentration occurring between 24 and 48 hours. In both experiments, we used five technical replicates for each of the timepoints, resulting in a total of 50 samples per experiment. Timepoint 0 was approximately 30-60 minutes post blood collection.

2.2 RNA extraction

We extracted total RNA from the deposited blood using the PureLink Total RNA Blood Purification kit by Invitrogen [49]. Due to the potential of blood clotting, we doubled the volume of lysis buffer (L5) recommended in the manufacturer's protocol. We also completed an optional on-column DNase incubation following the manufacturer's protocol. Total RNA was eluted with 30 µl of RNase-free water and prepared for analysis on the Agilent Technologies 4200 TapeStation [50]. Following the manufacturer's protocol for the *High Sensitivity RNA ScreenTape Assay Quick Guide*, we mixed 1 µl of the high sensitivity RNA screen tape sample buffer with 2 µl of the total RNA extracts [50]. Samples were briefly centrifuged before testing with the TapeStation. Following TapeStation analysis, we collected and examined a series of RNA metrics using the TapeStation Analysis Software A.02.02. One such metric, the RINe, is generated by an algorithm that calculates its value for the total RNA based on the ratio of the height of the 18S rRNA peak to the background signal, which represents the signal for fragments found in the fast zone ranging from 200 bp to 1.8 kb [51,52]. It is a dimensionless

variable that ranges from 1 to 10, with 10 representing intact and high-quality RNA, while a value of 1 represents low-quality and highly fragmented RNA [51,53]. In addition to the default metrics given by the instrument, such as RINe, concentration, 28S and 18S peak concentrations, we inserted a new peak ranging from 200 bp to 500 bp, which should represent the smaller mRNAs in our samples [54].

2.3 Statistical analyses

Correlation matrices were built prior to modelling to ensure that the response variables (RNA metrics) included in the analyses were not highly correlated to each other (Pearson's r < abs(0.70)). The retained RNA metrics were subject to linear regressions while using log-transformed time as the explanatory variable. As our first timepoint was 0 hours, which is a value that cannot be log-transformed, we assigned it a value of 0.1 (6 minutes) prior to the transformation. Slope, R^2 and p-values were recorded for each regression. Variables showing independence and a correlation to time were used to build a series of linear mixed-effects models, with donor (individual cow) acting as a random effect. Each donor represents a separate experiment.

After preliminary analysis of our data, we were interested in a shift in RNA metrics that was apparent after 24 hours. Following the assessment of our data's normality using the Shapiro-Wilk test, we applied the unpaired two-samples Wilcoxon test, a non-parametric test, to determine whether there was a significant difference in our response variables before and after the shift occurring at 24 hours. This test determines whether the means of two independent samples are significantly different from each other. Principal component analysis

(PCA) was used to integrate and visualize the uncorrelated metrics. All statistical analyses and data visualizations were created using R Version 4.0.3.

3. Results

We collected eight RNA metrics following the analysis of total RNA with the 4200 TapeStation; of these, three were retained for further statistical analyses, as they were not correlated to each other (Pearson's r < abs(0.70)) (Fig. 1). The retained metrics included the RINe, total RNA concentration and 28S/18S rRNA peak area ratio (Table 1). Statistics for all eight RNA metrics can be found in the supplemental material (Table S1).

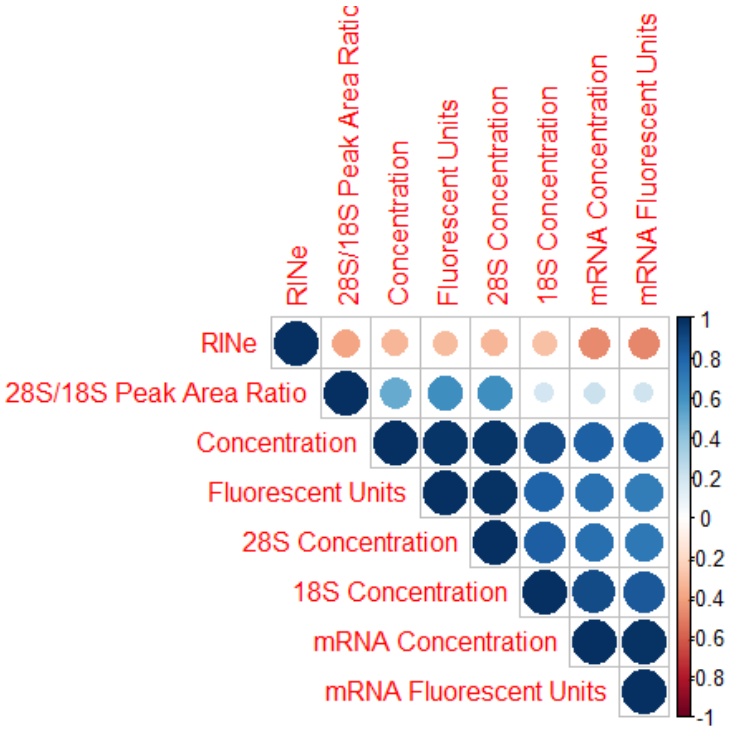

Fig. 1. Correlations between the eight RNA metrics obtained from the 4200 TapeStation RNA analysis. Size of the dot increases with a greater correlation between variables. Blue-coloured dots indicate a positive correlation between RNA metrics, while red-coloured dots indicate a negative correlation between them. Shading of the dot increases with a greater correlation, with light colours indicating a weak correlation and darker colours indicating a strong

217 correlation (see legend). RINe is the only metric to exhibit a negative correlation with another
218 variable.

219 **Table 1:** Statistics for the linear regressions of the three retained RNA metrics against log-
220 transformed time. Significant p-values are bolded. Donor was used as a random effect.

Log(Time)					
RNA metrics	**Marginal R^2**	**Conditional R^2**	**Estimate**	**Confidence Interval**	**p-value**
RINe	0.696	0.712	-0.55	-0.62 – -0.48	**<0.001**
Concentration	0.087	0.211	-908.31	-1450.76 – -365.86	**0.001**
28S/18S Peak Area Ratio	0.054	0.118	0.39	-0.04 – 0.82	0.077

221

222 *3.1 RNA Integrity Number equivalent*

223 The RINe metric demonstrated the best fit model with time based on its R^2 (Table 1).
224 The addition of donor as a random effect in the linear mixed-effects model had little influence
225 on the model's goodness-of-fit, as seen in the slight differences in the marginal R^2 (no random
226 effect) and conditional R^2 (with random effect; Table 1). Samples from both donors exhibited a
227 clear and parallel negative trend over time, with no significant differences between donors (W
228 = 1029.5, p-value = 0.172) (Fig. 2). Visualization of the principal component analysis also
229 supported the lack of significant differences between donors (Fig. S1). Of note, both donors
230 exhibited a steep decrease in RINe values after 24 hours, at which point there was no further
231 significant increase or decrease in the RINe for either donor. The unpaired Wilcoxon test found
232 a statistically significant difference in the RINe values before and after 24 hours (Donor A; W =
233 572.5, p-value < 0.0001, Donor B; W = 586.5, p-value < 0.0001, combined; W = 2323, p-value <
234 0.0001).

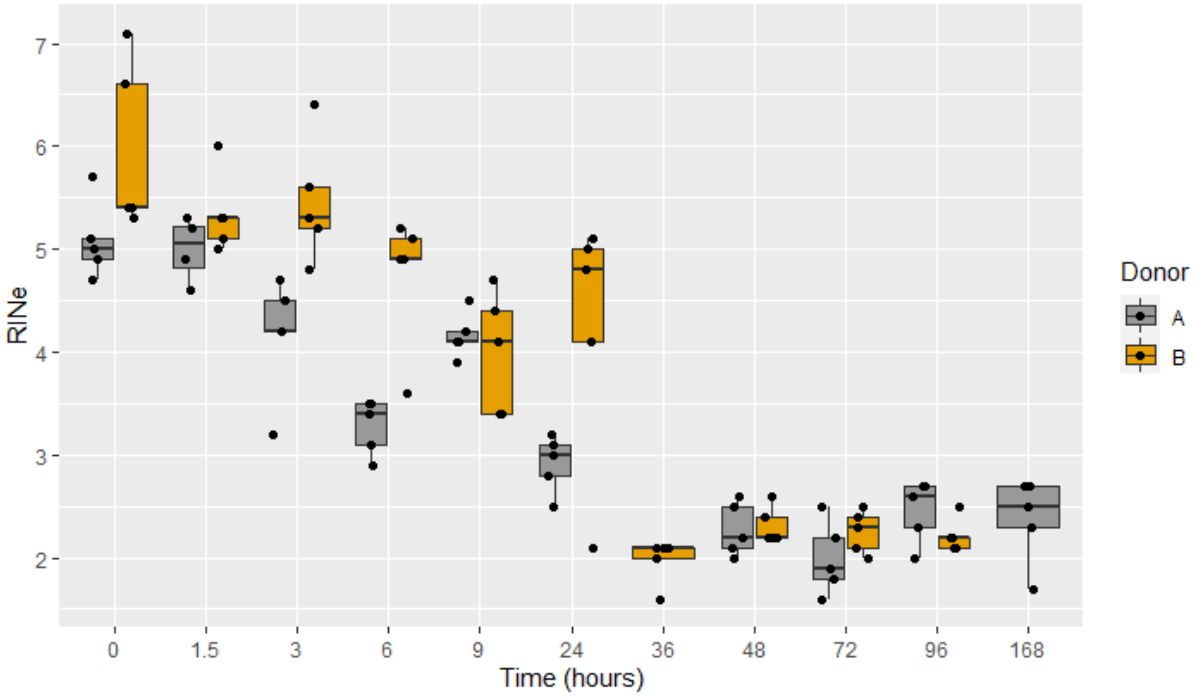

Fig. 2. Relationship between the RNA Integrity Number equivalent (RINe) and time. Donor A represents the first time-series experiment, conducted with blood from one cow. Donor B represents the second time-series experiment, conducted with blood from another cow. There is a negative association between the RINe and time. A sharp decrease in the RINe is observed after 24 hours. Note that the timepoints of 36 and 168 hours only consist of replicates from one donor.

3.2 Total RNA concentration

The concentration of total RNA was shown to have a weaker association with time when compared to the RINe (Table 1). In this case, the addition of donor as a random effect in the linear mixed-effects model more than doubled the model's fit (Table 1). Similarly to the RINe, total RNA concentration exhibited a negative trend over time, with greater concentrations at early timepoints and lower concentrations at later timepoints (Fig. 3). The unpaired Wilcoxon non-parametric test did find a significant difference between donor concentrations from

bloodstains deposited for 24 hours or less (W = 724, p-value <0.001). No significant difference was found between donor concentrations for bloodstains aged for more than 24 hours (W = 240, p-value = 0.2888). When considering the whole time series, a significant difference in total concentration was observed between donors (W = 1591.5, p-value = 0.010). Further, a significant decrease in total RNA concentration was observed after 24 hours for both donors (Donor A; W = 560, p-value <0.0001, Donor B; W = 578, p-value <0.0001, combined; W = 2240.5, p-value <0.0001). Concentrations above the 4200 TapeStation's limit of quantification (500 pg/µl) were recorded up to 24 hours, after which the majority of observations fell below this threshold but remained above the instrument's limit of detection (100 pg/µl). Replicates from the same donor displayed poor precision for most timepoints, with the time of initial pipetting and 36 hours being potential exceptions for donor B. The 24-hour timepoint concentrations for donor A ranged from 264 pg/µl to 19700 pg/µl. Concentrations for donor B at the same timepoint varied from 22 pg/µl to 6690 pg/µl.

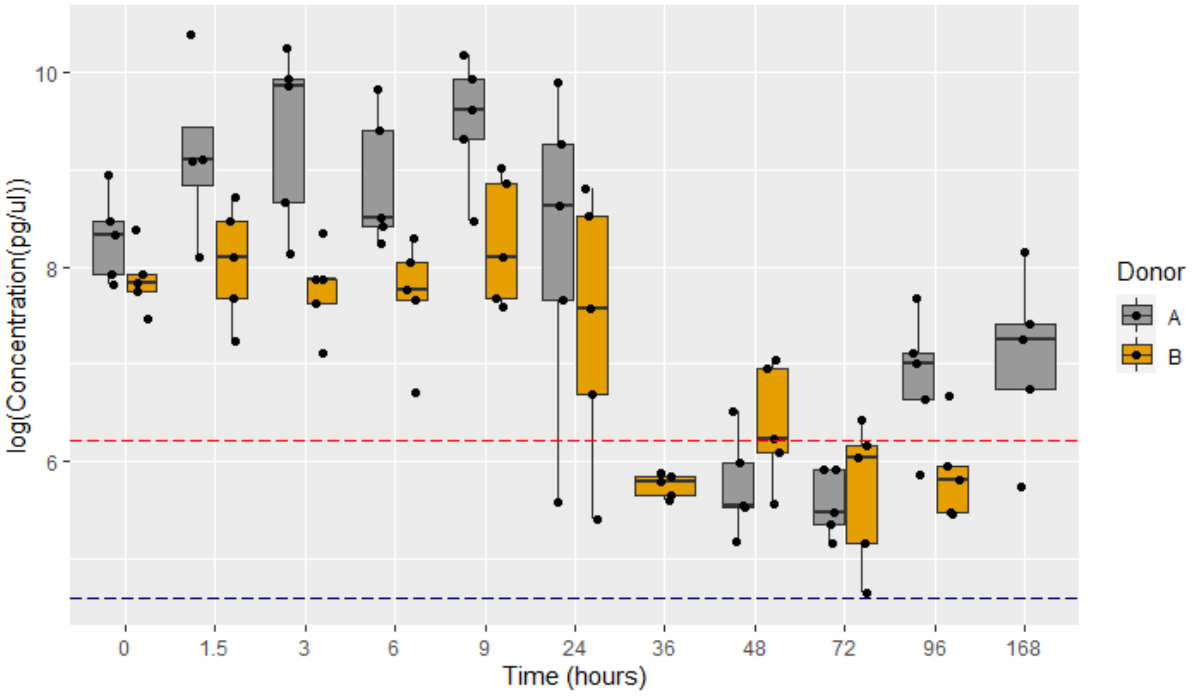

Fig. 3. Relationship between total RNA concentration and time. Concentration has been log-transformed for visualization purposes. The red dashed line represents the 4200 TapeStation's limit of quantification (500 pg/µl) and the navy dashed line represents the instrument's limit of detection (100 pg/µl). The most accurate quantification of total RNA concentration occurs while above the limit of quantification, but below 10000 pg/µl. The limit of detection is the lowest concentration at which the instrument can accurately detect total RNA. There is a negative trend between concentration and time, which can be seen in both donors. A significant decrease in concentration is observed after 24 hours.

The 28S/18S rRNA peak area ratio was the retained RNA metric that displayed the lowest association with time (Table 1). The addition of donor as a random effect in the linear mixed-effect model did increase the fit; however, both were still very low. Peak area ratios were only obtained for timepoints up to 9 hours for donor A and 24 hours for donor B (Fig. S2).

The 28S/18S peak area ratios could not be obtained for the later timepoints, as the 18S rRNA peak dropped out of the electropherograms and was no longer being called (Fig. S3).

4. Discussion

Estimating the age of biological fluids found at crime scenes, such as bloodstains, remains a challenge within the forensic community [1]. Methods have been developed in controlled laboratory settings, but none have been accepted for crime scene use due to insufficient sensitivity and high variability between samples [3,9–13,15]. Our study examined the degradation of total RNA present in bloodstains over 168 hours using the Agilent 4200 TapeStation, an instrument providing automated high-sensitivity RNA gel electrophoresis, in an attempt to uncover RNA metrics that could be used to accurately estimate the TSD of bloodstains. While we did observe time-dependent changes in some of the analyzed RNA metrics, there was high variability between technical replicates, similar to what was reported in Heneghan *et al.* [39]. However, even with this high variability, our results illustrate that the RINe metric, which normalized the discrepancies observed between donors for other RNA metrics, can be used as a diagnostic tool to differentiate day-old bloodstains from those that have been deposited for longer than 24 hours. The RINe metric demonstrated statistically significant changes after 24 hours of deposition.

From the retained RNA metrics, the RINe was the variable that demonstrated the greatest association with time, followed by total RNA concentration and 28S/18S rRNA peak area ratios (Table 1, Fig. 1). The model including RINe exhibited the greatest R^2, with and without donor (biological replicate) as a random effect (Table 1). Although the addition of donor as a random effect does not significantly increase the model's fit for RINe, it does

297 increase the fit for both total RNA concentration and 28S/18S rRNA peak area ratio (Table 1),
298 suggesting that the RINe is independent of biological replicate and negating the need for a
299 random effect while using this metric. Blood composition does vary by individual; in fact,
300 research on human blood discovered that the amount of RNA in healthy subjects varied from
301 6.7 to 22.7 µg/ml [55]. This variability could lead to significant differences in concentrations of
302 total RNA obtained from biological replicates, as we observed during our study. Although
303 including this source of endogenous variation as a random effect can account for intrinsic
304 biological differences, the RINe metric was not affected by these potential discrepancies (Table
305 1). The RINe is an RNA quality metric that is automatically generated and calculated by
306 obtaining a ratio of the 18S rRNA peak height to the signal present in the fast zone
307 (approximately 200 bp - 1.8 kb), which represents fragmented RNA [51]. It exhibits a negative
308 correlation with time, with a significant decrease occurring after 24 hours, which is likely the
309 result of the deformation of white blood cells transpiring during the clotting and complete
310 drying of the blood [45,46]. This was further accompanied by the dropout of the 18S rRNA
311 peak.

312 Bloodstains had completely dried out by 36 hours, at which point we observed a
313 decrease in the degradation rate of the RNA. As the time-series proceeded, we observed the
314 dropout of the 18S rRNA (Fig. S4); as this peak is important for the analyzed RNA quality
315 metrics, understanding the reasons for its dropout is crucial. This dropout could have been
316 caused by the fragmentation of the 18S rRNA via RNases, or by other exogenous means. RNases
317 cleave the phosphodiester bonds in RNA more effectively in hydrated environments, and the
318 DV200, the percentage of RNA fragments longer than 200 bp, decreased after 24 hours,

319 indicating that there had been an increase in small RNA fragments (Fig. S5) [28,56]. As the 28S
320 rRNA (4-5 kb depending on species) and 18S rRNA (1.8 kb) are the most abundant, and largest
321 types of RNA in white blood cells, it is possible that their fragmentation and degradation are the
322 main drivers in the observed decrease of the DV200 [28].

323 Although the term 'dropout' is used throughout, it may not be a proper description of
324 the 18S rRNA situation. The increase in signal from the fast zone, caused by an excess of small
325 fragments, may mask the 18S rRNA peak that would normally be called in their absence. As
326 larger RNA fragments are cleaved, the resulting smaller fragments accumulate in the fast zone,
327 a process that raises the fluorescent signal next to the 18S rRNA peak [52]. Additionally,
328 microbial contamination could be to blame for the masking of the 18S rRNA peak and the slight
329 increase in total RNA concentration at 168 hours. Microbial contamination of surfaces and
330 objects is expected to increase with longer amounts of time, as seen in Tamburini *et al.* [57]. A
331 longer period to interact with the surrounding environment could introduce foreign sources
332 into or onto the bloodstains. As the 16S bacterial rRNA is approximately 1.6 kb [58], it could be
333 detected, raising the background fluorescence next to the 18S rRNA peak, leading to its
334 masking. One of these factors, or most likely a combination of them, could have affected the
335 recovery of 18S rRNA from stains at later timepoints. Alternatively, the inadequate lysis of
336 white blood cells from the clotted blood could have led to the dropout of 18S rRNA, as well as
337 the sharp decreases that were seen in the RINe and total RNA concentration [59]. However, this
338 seems unlikely as the 28S rRNA peak was still present at later timepoints, indicating that RNA
339 could still be extracted successfully from the bloodstains, regardless of the clotting. It is
340 important to note that some of our samples underwent insufficient heat denaturation,

represented by the 28S rRNA double peaks in the electropherograms [51] (Fig. S6). As a result, 28S rRNA likely retained its secondary and tertiary structures, providing greater stability and resulting in less fragmentation over time [26]. Therefore, we suggest that the RNA fragmentation was biased towards the 18S rRNA.

As expected, the concentration of total RNA decreased over time. However, we expected the largest decrease to occur within the first 24 hours, mainly due to degradation via ubiquitously present enzymes. Concentration, however, remained stable within the first 24 hours and the largest decrease occurred after 24 hours with a sudden drop in concentration that fell below the TapeStation's quantitative range (lower limit of 500 pg/µl). Total RNA concentration was being driven by the quantity of 28S rRNA much more than it was by the 18S rRNA quantity. By observing the figures for total RNA concentration and 28S rRNA concentration over time, it is easy to note the resemblances in trends, especially during the first 24 hours (Fig. 3, Fig. S6). Both are relatively stable before 24 hours, exhibiting little variation. Visual differences in trends between the 18S rRNA concentration (Fig. S4) and 28S rRNA concentration (Fig. S6) also indicate that both rRNAs species are the subject of different degradation processes, further supporting the explanation that the 18S rRNA is undergoing greater enzymatic degradation.

As our approach analyzes total RNA rather than simply mRNA, conducting direct comparisons between our results and those obtained in previous studies can be difficult. Although trends in total RNA concentration tend to follow those found using mRNA transcripts, the latter is much more sensitive as its targeting a specific gene and can determine actual copy numbers [3,14,39]. Most studies use RT-qPCR to amplify the amount of mRNA transcripts

363 obtained from bloodstains, something that is not done in our study, which allows for a longer
364 time-series, and detection for much greater periods than what we observed. Fu *et* al.[14], as
365 well as Weinbrecht *et* al. [13], both detected blood-specific transcripts from bloodstains
366 deposited for up to one year, while the total RNA concentration in our study fell below the
367 quantitative range of the 4200 TapeStation after 24 hours of deposition. While qPCR can
368 quantify copy number, such a long-term persistence of mRNA is not concordant with our
369 current understanding of the molecule, as 80% of mRNAs have a half-life of 2 minutes or less
370 [60].

371 Due to the high variability between technical replicates, age estimations were not
372 conducted using any of our developed models. However, the sharp drop observed for the RINe
373 metric after 24 hours could allow for differentiation of day-old bloodstains from older
374 bloodstains. This is similar to a finding by Anderson *et al.* [3], where they differentiated
375 bloodstains deposited for 6 days from fresh blood and bloodstains aged for 30 days from those
376 deposited for 6 days. Our results are also similar to the findings of Cossette *et al.* [24], where
377 DNA allowed for the differentiation of fresh bloodstains from older bloodstains. The significant
378 decrease observed in RINe after 24 hours is a significant finding that warrants further research.
379 We note here that our use of technical and biological replicates demonstrated that our findings
380 were reproducible, suggesting this may indeed be a universal diagnostic signal.

381 Further, we have no reason to suspect that the patterns we observed would not be
382 present in human blood itself. Bovine blood, while mixed with ACD-A at 12.5% v/v, is a
383 validated human blood substitute, as it exhibits similar fluid properties to that of human blood
384 [47]. Additionally, we would not expect the ribosomal RNA to be affected by different agonal

states. Ribosomal RNA, namely 18S rRNA, is often used as a normalizer or reference gene due to its constitutive expression and ability to tolerate different stimuli [61]. Moving forward, future research should focus on experiments using the outlined methods to assess the repeatability of our findings. A larger number of technical and biological replicates could also be utilized to assess intra- and inter-donor variability. The effects of temperature, humidity and substrate on the results should also be evaluated. All three of these factors have been shown to affect the RNA degradation and drying times of bloodstains, which could cause the drop in RNA metrics to occur at earlier or later timepoints [20,38,39]. Further, the type of RNA extraction used could also influence the RNA yield. The PureLink Total RNA Blood Purification Kit used in this study required a minimal input of 50 µl of blood [49]. This can be considered a limitation, especially in crime scene scenarios in which there are only a few drops of blood. Therefore, different RNA extraction techniques, such as organic extractions using TRIzol, or other column-based techniques, such as RiboPure, PAXgene, RNeasy and LeucoLock should be used to conduct the study [62]. Schwochow *et al.* [62] have shown that the above methods do yield different integrity numbers and concentrations, indicating that extraction efficiencies are not homogenous across all methods.

5. Conclusion

Our study aimed to explore the potential use of total RNA degradation in bloodstain TSD models, either as a stand-alone or a complementary analysis. Our results demonstrated significant changes in the RINe and total RNA concentration of RNA extracted from bloodstains deposited for up to 168 hours. A significant decrease in the RINe was observed after 24 hours, suggesting that this could be used to differentiate day-old bloodstains from older bloodstains.

The two biological replicates that we included in this study produced similar results, indicating that this method was reproducible. However, high variability between technical replicates prevented accurate age estimates, demonstrating that this technique is not yet precise enough for crime scene use. Further research including a greater number of technical and biological replicates may aid in increasing the preciseness of this method. Different temperatures and substrates should also be used to mimic crime scene scenarios, broadening this technique's applicability. As of now, this method should not be used as a stand-alone model; rather, it should be combined with other analyses that have constructed more accurate and precise TSD models. This type of combinatorial research could bring the forensic community one step closer to developing a sensitive and robust TSD model for bloodstains that could one day be applied to crime scene samples.

Author Contributions

Colin Elliott: Visualization, Writing - original draft, Formal analysis, Investigation, Funding acquisition, Software, Data curation, Methodology. **Theresa Stotesbury**: Conceptualization, Supervision, Funding acquisition, Resources, Writing - review & editing, Project administration, Methodology, Validation. **Aaron B.A. Shafer**: Conceptualization, Supervision, Funding acquisition, Resources, Writing - review & editing, Project administration, Methodology, Validation.

Declaration of Competing Interest

The authors report no declarations of interest.

Acknowledgements

The authors would like to acknowledge Alon Gabriel, Jesse Wolf and Marie-Laurence Cossette of the Wildlife and Applied Genomics laboratory group at Trent University for their insights and feedback on writing, visualizations and statistical analyses. The authors would also like to thank Otonabee Meat Packers for providing the blood samples.

Funding

This work was supported by two NSERC Undergraduate Student Research Awards (Canada) and an NSERC Canada Graduate Scholarship – Master's program (Canada) to Colin I. Elliott, Natural Sciences and Engineering Research Council of Canada, Grant/Award Number: RGPIN-2017-03934 and Canadian Foundation for Innovation-JELF, Grant/Award Number: #36905 to Aaron B.A. Shafer.

References

[1] R.H. Bremmer, K.G. De Bruin, M.J.C. Van Gemert, T.G. Van Leeuwen, M.C.G. Aalders, Forensic quest for age determination of bloodstains, Forensic Sci. Int. 216 (2012) 1–11. https://doi.org/10.1016/j.forsciint.2011.07.027.

[2] G. Zadora, A. Menzyk, In the pursuit of the holy grail of forensic science - Spectroscopic studies on the estimation of time since deposition of bloodstains, Trends Anal. Chem. 105 (2018) 137-165. https://doi.org/10.1016/j.trac.2018.04.009.

[3] S.E. Anderson, G.R. Hobbs, C.P. Bishop, Multivariate analysis for estimating the age of a bloodstain, J. Forensic Sci. 56 (2011) 186–193. https://doi.org/10.1111/j.1556-4029.2010.01551.x.

[4] R. Steelberg, D.S. Pietro, A preliminary assessment of the correlation of drying time and

453 the peripheral rim thickness of perimeter bloodstains, J. Forensic Res. 10 (2019) 1-5.

454 [5] O. Peschel, S.N. Kunz, M.A. Rothschild, E. Mutzel, Blood stain pattern analysis, Forensic
455 Sci. Med. 7 (2011) 257–270. https://doi.org/10.1007/s12024-010-9198-1.

456 [6] M. Lynch, God's signature: DNA profiling, the new gold standard in forensic science,
457 Endeavour. 27 (2003) 93–97. https://doi.org/10.1016/S0160-9327(03)00068-1.

458 [7] J.M. Butler, Genetics and genomics of core short tandem repeat loci used in human
459 identity testing, J. Forensic Sci. 51 (2006) 253–265. https://doi.org/10.1111/j.1556-
460 4029.2006.00046.x.

461 [8] D.R. Hares, Selection and implementation of expanded CODIS core loci in the United
462 States, Forensic Sci. Int. Genet. 17 (2015) 33–34.
463 https://doi.org/10.1016/j.fsigen.2015.03.006.

464 [9] K.C. Doty, G. McLaughlin, I.K. Lednev, A Raman "spectroscopic clock" for bloodstain age
465 determination: the first week after deposition, Anal. Bioanal. Chem. 408 (2016) 3993–
466 4001. https://doi.org/10.1007/s00216-016-9486-z.

467 [10] E.K. Hanson, J. Ballantyne, A blue spectral shift of the hemoglobin Soret band correlates
468 with the age (time since deposition) of dried bloodstains, PLoS One. 5 (2010) 1–11.
469 https://doi.org/10.1371/journal.pone.0012830.

470 [11] J. Agudelo, C. Huynh, J. Halámek, Forensic determination of blood sample age using a
471 bioaffinity-based assay, Analyst. 140 (2015) 1411–1415.
472 https://doi.org/10.1039/c4an02269f.

473 [12] K. Lech, F. Liu, K. Ackermann, V.L. Revell, O. Lao, D.J. Skene, M. Kayser, Evaluation of
474 mRNA markers for estimating blood deposition time: Towards alibi testing from human
475 forensic stains with rhythmic biomarkers, Forensic Sci. Int. Genet. 21 (2016) 119–125.
476 https://doi.org/10.1016/j.fsigen.2015.12.008.

477 [13] K.D. Weinbrecht, J. Fu, M. Payton, R. Allen, Time-dependent loss of mRNA transcripts
478 from forensic stains, Res. Reports Forensic Med. Sci. 7 (2017) 1–12.
479 https://doi.org/10.2147/rrfms.s125782.

480 [14] J. Fu, R.W. Allen, A method to estimate the age of bloodstains using quantitative PCR,
481 Forensic Sci. Int. Genet. 39 (2019) 103–108.
482 https://doi.org/10.1016/j.fsigen.2018.12.004.

483 [15] S. Strasser, A. Zink, G. Kada, P. Hinterdorfer, O. Peschel, W.M. Heckl, A.G. Nerlich, S.
484 Thalhammer, Age determination of blood spots in forensic medicine by force
485 spectroscopy, Forensic Sci. Int. 170 (2007) 8–14.
486 https://doi.org/10.1016/j.forsciint.2006.08.023.

487 [16] C.S. Thom, C.F. Dickson, D.A. Gell, M.J. Weiss, Hemoglobin variants: Biochemical
488 properties and clinical correlates, Cold Spring Harb. Perspect. Med. 3 (2013) 1-22.
489 doi:10.1101/cshperspect.a011858.

[17] N. Laan, F. Smith, C. Nicloux, D. Brutin, Morphology of drying blood pools, Forensic Sci. Int. 267 (2018) 104–109.

[18] D. Brutin, B. Sobac, B. Loquet, J. Sampol, Pattern formation in drying drops of blood, J. Fluid Mech. 667 (2011) 85–95. https://doi.org/10.1017/S0022112010005070.

[19] J.P. Riddel Jr, B.E. Aouizerat, C. Miaskowski, D.P. Lillicrap, Theories of blood coagulation, J. Pediatr. Oncol. 24 (2007) 123–131. https://doi.org/10.1177/1043454206298693.

[20] T.L. Laber, B.P. Epstein, Substrate effects on the clotting time of human blood, J. Can. Soc. Forensic Sci. 34 (2001) 209–214. https://doi.org/10.1080/00085030.2001.10757531.

[21] J. Hansen, I. Lesnikova, DNA and RNA analysis of blood and muscle from bodies with variable postmortem intervals, Forensic Sci. Med. Pathol. 10 (2014) 322–328. https://doi.org/10.1007/s12024-014-9567-2.

[22] J. Dissing, A. Søndervang, S. Lund, Exploring the limits for the survival of DNA in blood stains, J. Forensic Leg. Med. 17 (2010) 392–396. https://doi.org/10.1016/j.jflm.2010.08.001.

[23] T. Stotesbury, M.L. Cossette, T. Newell-Bell, A.B.A. Shafer, An exploratory time since deposition analysis of whole blood using metrics of DNA degradation and visible absorbance spectroscopy, Pure Appl. Geophys. (2020). https://doi.org/10.1007/s00024-020-02494-0.

[24] M.L. Cossette, T. Stotesbury, A.B.A. Shafer, Quantifying visible absorbance changes and DNA degradation in aging bloodstains under extreme temperatures, Forensic Sci. Int. 318 (2021) e110627. https://doi.org/10.1016/j.forsciint.2020.110627.

[25] S.L. Fordyce, M.L. Kampmann, N.L. van Doorn, M.T.P. Gilbert, Long-term RNA persistence in postmortem contexts, Investig. Genet. 4 (2013) 1–7. https://doi.org/10.1186/2041-2223-4-7.

[26] J. Nowakowski, I. Tinoco, RNA Structure and Stability, Semin Virol 165 (1997) 153–165.

[27] J. Wu, J. Xiao, Z. Zhang, X. Wang, S. Hu, J. Yu, Ribogenomics: The science and knowledge of RNA, Genom. Proteom. Bioinf. 12 (2014) 57–63. https://doi.org/10.1016/j.gpb.2014.04.002.

[28] P. Natsidis, P.H. Schiffer, I. Salvador-Martínez, M.J. Telford, Computational discovery of hidden breaks in 28S ribosomal RNAs across eukaryotes and consequences for RNA integrity numbers, Sci. Rep. 9 (2019) 1–10. https://doi.org/10.1038/s41598-019-55573-1.

[29] M. Sidstedt, J. Hedman, E.L. Romsos, L. Waitara, L. Wadsö, C.R. Steffen, P.M. Vallone, P. Rådström, Inhibition mechanisms of hemoglobin, immunoglobulin G, and whole blood in digital and real-time PCR, Anal. Bioanal. Chem. 410 (2018) 2569–2583. https://doi.org/10.1007/s00216-018-0931-z.

[30] N. Minshall, A. Git, Enzyme- and gene-specific biases in reverse transcription of RNA raise concerns for evaluating gene expression, Sci. Rep. 10 (2020) 1–7.

https://doi.org/10.1038/s41598-020-65005-0.

[31] S.G. Acinas, R. Sarma-Rupavtarm, V. Klepac-Ceraj, M.F. Polz, PCR-induced sequence artifacts and bias: Insights from comparison of two 16s rRNA clone libraries constructed from the same sample, Appl. Environ. Microbiol. 71 (2005) 8966–8969. https://doi.org/10.1128/AEM.71.12.8966-8969.2005.

[32] W. Yang, Nucleases: Diversity of structure, function and mechanism, Q. Rev. Biophys. 44 (2011). https://doi.org/10.1017/S0033583510000181.

[33] H. Tani, H. Sato, M. Torimura, Rapid monitoring of RNA degradation activity in vivo for mammalian cells, J. Biosci. Bioeng. 123 (2017) 523–527. https://doi.org/10.1016/j.jbiosc.2016.11.010.

[34] T. Miyamoto, S. Okano, N. Kasai, Irreversible thermoinactivation of ribonuclease-A by soft-hydrothermal processing, Biotechnol. Prog. 25 (2009) 1678–1685. https://doi.org/10.1002/btpr.267.

[35] M. Vennemann, A. Koppelkamm, Postmortem mRNA profiling II: Practical considerations, Forensic Sci. Int. 203 (2010) 76–82. https://doi.org/10.1016/j.forsciint.2010.07.007.

[36] L.L. Yan, H.S. Zaher, How do cells cope with RNA damage and its consequences?, J. Biol. Chem. 294 (2019) 15158–15171. https://doi.org/10.1074/jbc.REV119.006513.

[37] E.J. Wurtmann, S.L. Wolin, RNA under attack: Cellular handling of RNA damage, Crit. Rev. Biochem. Mol. Biol. 44 (2009) 34–49. https://doi.org/10.1080/10409230802594043.

[38] M. Sirker, P.M. Schneider, I. Gomes, A 17-month time course study of human RNA and DNA degradation in body fluids under dry and humid environmental conditions, Int. J. Legal Med. 130 (2016) 1431–1438. https://doi.org/10.1007/s00414-016-1373-9.

[39] N. Heneghan, J. Fu, J. Pritchard, M. Payton, R.W. Allen, The effect of environmental conditions on the rate of RNA degradation in dried blood stains, Forensic Sci. Int. Genet. 51 (2021) 102456. https://doi.org/10.1016/j.fsigen.2020.102456.

[40] H.S. Bernhardt, W.P. Tate, Primordial soup or vinaigrette: Did the RNA world evolve at acidic pH?, Biol. Direct. 7 (2012) 4-15. https://doi.org/10.1186/1745-6150-7-4.

[41] I.B. Slimen, T. Najar, A. Ghram, H. Dabbebi, B. Mrad, M. Abdrabbah, Reactive oxygen species, heat stress and oxidative-induced mitochondrial damage. A review, Int. J. Hyperther. 30 (2014) 513-523. https://doi.org/10.3109/02656736.2014.971446.

[42] M. Setzer, J. Juusola, J. Ballantyne, Recovery and stability of RNA in vaginal swabs and blood, semen, and saliva stains, J. Forensic Sci. 53 (2008) 296–305. https://doi.org/10.1111/j.1556-4029.2007.00652.x.

[43] E. Hanson, S. Ingold, C. Haas, J. Ballantyne, Messenger RNA biomarker signatures for forensic body fluid identification revealed by targeted RNA sequencing, Forensic Sci. Int. Genet. 34 (2018) 206–221. https://doi.org/10.1016/j.fsigen.2018.02.020.

[44] M. Bauer, RNA in forensic science, Forensic Sci. Int. Genet. 1 (2007) 69–74. https://doi.org/10.1016/j.fsigen.2006.11.002.

[45] A. Pal, A. Gope, G. Iannacchione, Temperature and concentration dependence of human whole blood and protein drying droplets, Biomolecules. 11 (2021) 1–18. https://doi.org/10.3390/biom11020231.

[46] A. Pal, A. Gope, J.D. Obayemi, G.S. Iannacchione, Concentration-driven phase transition and self-assembly in drying droplets of diluting whole blood, Sci. Rep. 10 (2020) 1–12. https://doi.org/10.1038/s41598-020-76082-6.

[47] A. Orr, R. Gualdieri, M.L. Cossette, A. Shafer, T. Stotesbury, Whole bovine blood use in forensic research: Sample preparation and storage considerations, Sci. Justice. (2021). https://doi.org/10.1016/j.scijus.2021.02.004.

[48] C.E. Giraldo, M.E. Álvarez, J.U. Carmona, Effects of sodium citrate and acid citrate dextrose solutions on cell counts and growth factor release from equine pure-platelet rich plasma and pure-platelet rich gel, BMC Vet. Res. 11 (2015) 1–7. https://doi.org/10.1186/s12917-015-0370-4.

[49] Invitrogen Life Technologies, PureLink ^{TM} total RNA blood purification kit: for isolating total RNA from whole blood, (2005).

[50] Agilent Technologies, Agilent high sensitivity RNA screentape system quickguide, (n.d.).

[51] Agilent Technologies, Agilent 4200 TapeStation system: system manual, (n.d.).

[52] Agilent Technologies, Comparison of RIN and RINe algorithms for the Agilent 2100 Bioanalyzer and the Agilent 2200 TapeStation systems, (n.d.) 1–4.

[53] A. Schroeder, O. Mueller, S. Stocker, R. Salowsky, M. Leiber, M. Gassmann, S. Lightfoot, W. Menzel, M. Granzow, T. Ragg, The RIN: an RNA integrity number for assigning integrity values to RNA measurements, BMC Mol. Biol. 14 (2006) 1–14. https://doi.org/10.1186/1471-2199-7-3.

[54] A. Piovesan, M. Caracausi, F. Antonaros, M.C. Pelleri, L. Vitale, GeneBase 1.1: A tool to summarize data from NCBI gene datasets and its application to an update of human gene statistics, Database. 2016 (2016) 1–13. https://doi.org/10.1093/database/baw153.

[55] P. Chomczynski, W.W. Wilfinger, H.R. Eghbalnia, A. Kennedy, M. Rymaszewski, K. Mackey, Inter-individual differences in RNA levels in human peripheral blood, PLos One. 11 (2016) 1–15. https://doi.org/10.1371/journal.pone.0148260.

[56] I. Wimmer, A.R. Tröscher, F. Brunner, S.J. Rubino, C.G. Bien, H.L. Weiner, H. Lassmann, J. Bauer, Systematic evaluation of RNA quality, microarray data reliability and pathway analysis in fresh, fresh frozen and formalin-fixed paraffin-embedded tissue samples, Sci. Rep. 8 (2018) 1–17. https://doi.org/10.1038/s41598-018-24781-6.

[57] E. Tamburini, V. Donegà, M.G. Marchetti, P. Pedrini, C. Monticelli, A. Balbo, Study on microbial deposition and contamination onto six surfaces commonly used in chemical

and microbiological laboratories, Int. J. Environ. Res. Public Health.12 (2015) 8295–8311. https://doi.org/10.3390/ijerph120708295.

[58] Y.S. Bukin, Y.P. Galachyants, I. V. Morozov, S. V. Bukin, A.S. Zakharenko, T.I. Zemskaya, The effect of 16s rRNA region choice on bacterial community metabarcoding results, Sci. Data. 6 (2019) 1–14. https://doi.org/10.1038/sdata.2019.7.

[59] Z. Zakaria, S.H. Umi, S.S. Mokhtar, U. Mokhtar, M.Z. Zaiharina, A.T.A. Aziz, B.P. Hoh, An alternate method for DNA and RNA extraction from clotted blood, Genet. Mol. Res. 12 (2013) 302–311. https://doi.org/10.4238/2013.February.4.4.

[60] A. Baudrimont, S. Voegeli, E.C. Viloria, F. Stritt, M. Lenon, T. Wada, V. Jaquet, A. Becskei, Multiplexed gene control reveals rapid mRNA turnover, Sci. Adv. 3 (2017) 1-12. doi:10.1126/sciadv.1700006.

[61] G. Piazza, A. Bartke, J.G. Miquet, A.I. Sotelo, Analysis of different approaches for the selection of reference genes in RT-qPCR experiments: A case study in skeletal muscle of growing mice, Int. J. Mol. Sci. 18 (2017) 1-20. https://doi.org/10.3390/ijms18051060.

[62] D. Schwochow, L.E.K. Serieys, R.K. Wayne, O. Thalmann, Efficient recovery of whole blood RNA - a comparison of commercial RNA extraction protocols for high-throughput applications in wildlife species, BMC Biotechnol. 12 (2012) 1-12. doi: 10.1186/1472-6750-12-33.